Int. J. Heat Mass Transfer. Vol. 34, No. 3, pp. 723–738, 1991
Printed in Great Britain

0017–9310/91 $3.00 + 0.00

CHF behaviour during pressure, power and/or flow rate simultaneous variations

G. P. CELATA, M. CUMO, F. D'ANNIBALE, G. E. FARELLO and A. MARIANI
ENEA Casaccia, TERM/ISP Heat Transfer Laboratory, Via Anguillarese, 301, 00060 Rome, Italy

(*Received* 10 *October* 1989)

Abstract—The results of an experimental investigation are presented on critical heat flux in forced convective flow boiling during transients caused by simultaneous variations of either two or three parameters among pressure, flow rate and thermal power. The three parameters are varied according to an exponential law for the flow rate and the pressure decrease, and to a ramp and a step law for the input power increase. Experiments are carried out employing a tubular test section which is electrically and uniformly heated. Test parameters include the flow rate half-flow decay time, several values of the initial power (before the transient) and the final power (at the end of the transient) in the case of step transients, and the slope of the ramp in the case of ramp transients, and the depressurization rate. An analysis of the experimental data is performed using the local conditions approach, and applying the quasi-steady-state method. The effect of the simultaneous variation of either two or three main parameters on the time-to-crisis is also analysed for transients in which only one of the parameters is varied.

INTRODUCTION

THE CRITICAL heat flux (CHF) phenomenon has been extensively investigated in the past with particular regard to steady-state nuclear reactor operating conditions [1–5], with the aim of establishing the boundary conditions of the thermohydraulic design.

However, transient CHF is of great importance for the analysis of the thermohydrodynamic characteristics of petrochemical and nuclear power plants. In fact it is very likely to occur during off-normal conditions. An accurate knowledge of the transient CHF is needed for safety evaluations of the plants under accident conditions.

There are three different main types of transients: flow rate transients, pressure transients and power transients. From the viewpoint of plant safety the following variations with time are of interest: flow rate decrease, pressure decrease and power increase.

These three types of transients generally take place at the same time during plant accidents, and the situation becomes more complicated. It is therefore important, from an experimental point of view, to carry out tests in which all the three parameters potentially involved in the real accident transient are varied simultaneously in order to have the best representation of such transients. It will then be possible to verify the computation methods against an experimental data set which could be as close as possible to the real situation.

Transient boiling experiments in which only one parameter (flow rate, pressure or power) was varied, the other two being kept constant, have been extensively performed in the past. A thorough review was published by Kataoka and Serizawa [6].

Moxon and Edwards [7] carried out a series of experiments on forced convective transient boiling of water at a pressure of 6.9 MPa in step power increase and gradual flow decay (L/D = 200–400). Gaspari *et al.* [8] conducted an experiment on flow and power transients, using a 4 m long annulus (21 mm i.d. × 13.5 mm o.d.) with the outer tube heated. Water was circulated at 5 MPa. Shiralkar *et al.* [9] measured the transient time-to-crisis in a flow transient test, using water at 6.9 MPa flowing in a 2.7 m long annulus of 31.4 mm i.d. × 13.7 mm o.d. with the inner tube heated. Smirnov *et al.* [10, 11] studied experimentally the effect of the rate of inlet velocity decrease on the transient CHF velocity, using 1.4 and 0.5 mm long i.d., single tubes in water at 9.8 MPa. Iwamura and Kuroyanagi [12] carried out flow transient tests by linearly decreasing the inlet velocity of water flowing in a 0.8 m long, 10 mm i.d. tube at a pressure of 0.5–3.9 MPa. A similar experiment was conducted [13] with a higher rate of decrease, using Freon 12 flowing at a pressure of 1.1–1.8 MPa in a 2 m long, 7.8 mm i.d. tube. Leung [14, 15] measured the transient time-to-crisis for flow transients with Freon 11 flowing in a uniformly or non-uniformly heated tube (11.7 mm i.d., 3.05 mm long). Experiments were carried out [16–18] with exponential flow decrease, exponential pressure decrease and step or ramp power increase using Freon 12 flowing at pressures of 1.0–3.0 MPa in a 2.3 m long, 7.7 mm i.d. tube. Recently the CHF during transients caused by the simultaneous variation of two parameters—power (increase) and flow rate (decrease)—was studied [19]. Differences from 'single parameter' experiments were outlined and the quasi-steady-state method was proved successful in predicting the results.

The aim of the present paper is to describe a series of experiments carried out with Freon 12 to analyse

NOMENCLATURE

a_1, a_2	constants in equation (2) [s^4, s^3]
a	parameter in equation (1) [dimensionless]
b_1, b_2	constants in equation (2) [s^4, s^3]
b	parameter in equation (1) [m]
B	constant in equation (3) [s^{-1}]
c_1, c_2	constants in equation (4) [s^4, s^3]
c_p	liquid specific heat [J kg^{-1} K^{-1}]
d_1, d_2	constants in equation (4) [s^4, s^3]
D	diameter of test section [m]
E	excess to the crisis power [W]
G	mass flux [kg m^{-2} s^{-1}]
h	heat transfer coefficient [W m^{-2} K^{-1}]
h_{fg}	latent heat [J kg^{-1}]
L	length of heated test section [m]
M	margin to the crisis power [W]
p	pressure [Pa]
q''	heat flux [W m^{-2}]
S	wall/fluid heat transfer surface [m^2]
t	time [s]
T	temperature [°C]
V	volume of the test section wall [m^3]
x	steam quality [dimensionless]
W	thermal power [W].

Greek symbols

α	ramp slope [W s^{-1}]
β_1, β_2	parameters in equation (2) [s^{-1}]
γ_1, γ_2	parameters in equation (5) [s^3, s^3]
Γ	mass flow rate [kg s^{-1}]
$\varepsilon_1, \varepsilon_2$	parameters in equation (5) [s^3, s^2]
λ	parameter in equation (5) [s^{-1}]
λ_1, λ_2	parameters in equation (4) [s^{-1}]
ρ	density [kg m^{-3}].

Subscripts

b	bulk fluid
CHF	critical heat flux, thermal crisis
crit	critical condition
exp	experimental
f	liquid
h	half-flow
in	inlet
m	metal
o	situation before the transient
r	reduced
ss	steady-state
sub	subcooling
tr	transient
w	test section wall
∞	situation at the end of the transient.

the behaviour of CHF during transients caused by the simultaneous variation of either two or three of the parameters: flow rate, pressure and power, namely flow rate pressure transients, pressure power transients, pressure power flow rate transients. The variations studied correspond closely to the real situation of a plant accident, so the experiments permit an accurate assessment of methods employed in safety codes.

Data analysis was based on local condition analysis, and the quasi-steady-state method applied with acceptable results.

THE EXPERIMENTAL APPARATUS

The experimental R-12 loop is schematically illustrated in Fig. 1. It consists of a piston pump, a fluid-to-fluid pre-heater to control the inlet fluid temperature, a water cooled condenser and an R-12 tank. The use of R-12 as a test fluid allows the simulation of water at higher pressures and over a wider range of system parameter. The maximum operating pressure of the loop is 3.5 MPa, whereas the maximum mass flux is 1800 kg m^{-2} s^{-1}. The available electric power is 5 kW for the electric pre-heater and 10 kW for the test section.

The test section is a stainless steel tube uniformly and electrically heated over a length of 2.30 or 1.18 m, 7.7 mm in diameter. Its thermal diffusivity is about 4.1×10^{-6} m^2 s^{-1}. The test section instrumentation consists of 0.5 mm K-type thermocouples inserted into the tube wall and distributed as shown in Fig. 1. There are 12 wall and 6 bulk fluid temperature measuring stations available on the test section. The onset of the CHF condition is indicated by the thermocouple placed at the test section end, where the fluid exits from the tube. Tests carried out using a Wheatstone bridge did not give results different from those obtained with the thermocouple indication. R-12 flow is upwards with subcooled inlet conditions. Data acquisition is by a Computer DIGITAL MICRO PDP 11, coupled with an eight channel graphic Multirecorder Watanabe System.

EXPERIMENTAL RESULTS

Steady-state critical heat flux experiments

In order to establish the reference conditions for transients analysis, we first carried out a set of steady-state CHF tests [20].

In this investigation the pressure ranged from 1.25 MPa (corresponding to 8 MPa for water) to 2.75 MPa (corresponding to 16.2 MPa for water), whereas the mass flux ranged from 400 to 1600 kg m^{-2} s^{-1}. The inlet subcooling varied from 23 to 0°C.

Very few correlations are available in the literature

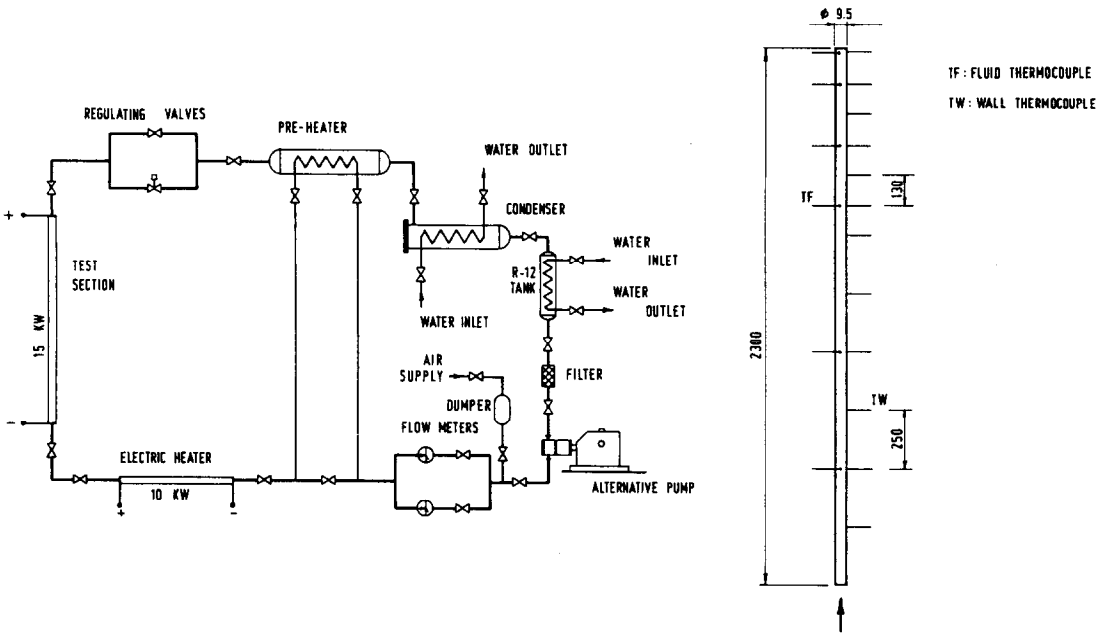

FIG. 1. Schematic of the experimental loop and the test section.

for CHF predictions with R-12 [20]. A correlation, proposed by Bertoletti *et al.* [21] for both water and R-12, has been adopted for the present study. It was slightly modified to have a better fit with the experimental data. The correlation has the following form (SI units):

$$q''_{CHF} = \frac{\Gamma h_{fg}}{\pi DL}\frac{(a - x_{in})}{\left(1+\frac{h}{L}\right)}$$

$$a = \frac{10(1.18 - 2.07P_r + 1.55P_r^2)}{G^{0.33}}$$

$$b = 0.3786\left(\frac{1}{P_r} - 1\right)^{0.4} D^{1.4}G \qquad (1)$$

where P_r is the reduced pressure, i.e. the ratio of the operating pressure, p, to the critical value, p_{crit} ($p_{crit} = 4.2$ MPa).

The comparison between the steady-state CHF experimental data and predictions obtained using the above correlation is shown in Fig. 2 for a mass flux ranging from 350 to 1500 kg m^{-2} s^{-1}. As shown in the figure, this agreement is good and within $\pm 10\%$ for 96% of the experimental data.

Test matrix

Transients with simultaneous variation of mass flow rate, pressure and thermal power involved three independent parameters: the initial pressure, p_o, the mass flux before the transient, G_o, and the thermal

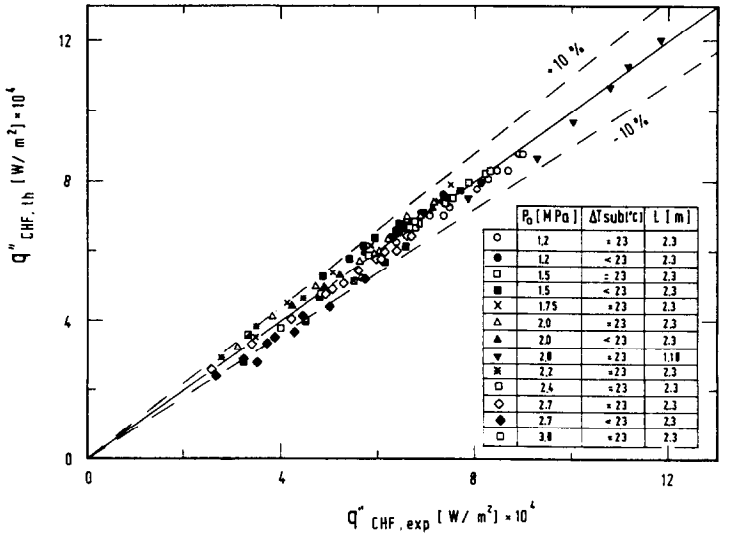

FIG. 2. Steady-state reference CHF tests: predictions obtained using correlation (1).

power input before the transient, W_o. The transient is described by several parameters. The mass flux decrease is characterized by the half-flow decay time, t_h, i.e. the time necessary to half the initial value, G_o. The step thermal power increase is characterized by the thermal power input at the end of the transient, W_∞. The ramp thermal power increase is characterized by the slope of the straight line to which the power ramp tends, α [kW s^{-1}]. The pressure decrease is characterized by the average pressure gradient over the first 0.5 s from the beginning of the transient, dp/dt (it is a reference value to compare different depressurization rates).

The inlet subcooling is kept constant during the tests.

(a) Transients with simultaneous variation of flow rate and pressure

The test matrix can be represented as follows:

p_o	[MPa]	1.25, 2.02
G_o	[kg m^{-2} s^{-1}]	1470
dp/dt	[MPa s^{-1}]	0.02, 0.05, 0.1, 0.2, 0.3
t_h	[s]	0.5
M	[kW]	0.5, 1.7.

The parameter M, which is defined as 'margin to the CHF', is linked to the initial value of the input power, W_o. It is the difference between the steady-state thermal crisis power, $W_{CHF,ss}$ and W_o (with the same values of G and p).

(b) Transients with simultaneous variation of pressure and heat flux (step and ramp variations)

The test matrix can be represented as follows:

p	[MPa]	202
G_o	[kg m^{-2} s^{-1}]	1470
dp/dt	[MPa s^{-1}]	0.02, 0.05, 0.1, 0.2, 0.3.

The values of thermal powers W_o and W_∞ are linked to W_{CHF}, p_o, and G, W_{CHF} being the steady-state critical thermal power calculated before the beginning of the transient. These latter values are reported in Table 1.

The values of W_o were fixed such that the difference between W_{CHF} and W_o (margin to the crisis, M) was constantly equal to either 0.5 or 1.7 kW. Similarly the value of W_∞, for step power variations, was chosen such that the difference between W_∞ and W_{CHF} (excess to the crisis, E) was always equal to 1.0 kW.

In the case of ramp variations of the power, α was

$$\alpha\ [\text{kW s}^{-1}] \quad 0.7, 1.9.$$

Table 1. Experimental steady-state CHF data

p [MPa]	G [kg m^{-2} s^{-1}]	W_{CHF} [W]
1.20	1470	5020
2.02	1470	4160

(c) Transients with simultaneous variation of pressure, flow rate and heat flux (step and ramp variations)

The test matrix can be represented as follows:

p_o	[MPa]	1.25, 2.02, 2.77
G_o	[kg m^{-2} s^{-1}]	1470
dp/dt	[MPa s^{-1}]	0.06, 0.09, 0.14, 0.29, 0.32
t_h	[s]	0.4
M	[kW]	0.5, 1.7.

For what concerns M, E and α, we employed the same values as point (b).

Transients characterization

Mass flow rate decays were obtained by means of a hydraulic integrator, made up with a regulating valve and a bleed controlled with pressurized air: higher pressures correspond to longer half-flow decay times, t_h.

Decay curves of inlet mass flux are approximated by the following mathematical expression:

$$\frac{G(t)}{G_0} = \beta_1^2\beta_2^2[(a_1+ta_2)\exp(\beta_1 t) + (b_1+tb_2)\exp(\beta_2 t)] \quad (2)$$

with

$$a_1 = -\left[\frac{2}{[\beta_1(\beta_1-\beta_2)^3]} + \frac{1}{[\beta_1^2(\beta_1-\beta_2)^2]}\right]$$

$$a_2 = \frac{1}{\beta_1(\beta_2-\beta_1)^2}$$

$$b_1 = -\left[\frac{2}{[\beta_2(\beta_2-\beta_1)^3]} + \frac{1}{[\beta_2^2(\beta_2-\beta_1)^2]}\right]$$

$$b_2 = \frac{1}{\beta_2(\beta_2-\beta_1)^2}$$

where β_1 and β_2 are values linked to the hydraulic integrator, obtained with best-fit procedures on experimental data of G [22].

Pressure decays were obtained by opening a regulating valve placed in the bypass line to the normal regulating valve. Decay curves of pressure are approximated by the following mathematical expression:

$$p(t) = p_o - p_\infty[1-\exp(-Bt)+(0.5B^2t^2+1)]. \quad (3)$$

Parameters B and $\Delta p = p_o - p_\infty$, obtained with a best-fit procedure, are reported in ref. [22]. The step thermal power input to the test section during a transient is not, however, of a step nature, owing to the finite time constants of the electric power system. The time-dependent expression of the step input power to the test section wall, $W(t)$, is approximated by the following expression:

$$W(t) = W_\infty + \lambda_1^2\lambda_2^2(W_\infty - W_o)[(c_1+tc_2)\exp(\lambda_1 t) + (d_1+td_2)\exp(\lambda_2 t)] \quad (4)$$

with

$$c_1 = -\left[\frac{2}{[\lambda_1(\lambda_1-\lambda_2)^3]} + \frac{1}{[\lambda_1^2(\lambda_1-\lambda_2)^2]}\right]$$

$$c_2 = \frac{1}{\lambda_1(\lambda_2-\lambda_1)^2}$$

$$d_1 = -\left[\frac{2}{[\lambda_2(\lambda_2-\lambda_1)^3]} + \frac{1}{[\lambda_2^2(\lambda_2-\lambda_1)^2]}\right]$$

$$d_2 = \frac{1}{\lambda_2(\lambda_2-\lambda_1)^2}$$

where λ_1 and λ_2 were determined through a best-fit procedure on the experimental data points [22].

In the case of the ramp input power variation, the time-dependent expression, $W(t)$, is approximated by the following expression:

$$W(t) = W_o + \alpha\lambda^2[(\varepsilon_1+\varepsilon_2 t)\,e^{\lambda t} + (\gamma_1+\gamma_2 t)] \quad (5)$$

where

$$\varepsilon_1 = -\frac{2}{\lambda^3}; \quad \varepsilon_2 = \frac{1}{\lambda^2}, \quad \gamma_1 = \frac{2}{\lambda^3}; \quad \gamma_2 = \frac{1}{\lambda^2}.$$

The value of λ was obtained by a best-fit procedure on the experimental data points [22]. The parameter α, is defined as the slope of $W(t)$ for $t > 3|\lambda|$; after this time the curve can be considered a straight line. In mathematical terms

$$\alpha = \left[\frac{dW}{dt}\right]_{t\Rightarrow\infty}.$$

The electrical power is read by instruments directly at the terminals placed on the test channel ends: therefore it is always exactly the thermal power that is being delivered to the wall. Computerized data acquisition takes into account the heat loss from the test section, which (although very small) was experimentally determined as a function of the wall temperature. Consequently $W(t)$ represents the actual net thermal power delivered to the test channel wall. The actual thermal power delivered to the fluid, W_f, depends not only on the response of the electric power system as discussed above, but also on the thermal capacity of the test section wall. Assuming that the test channel can be characterized by an average temperature T_w, we may write

$$W_f(t) = W(t) - (\rho c_p V)_m \frac{dT_w}{dt} \quad (6)$$

where ρ is the density, c_p the specific heat, and V the volume of the test section tube wall. Since the heat flux to the fluid may also be expressed in terms of the heat transfer coefficient from the wall to the fluid, h, heat transfer area, S, and the bulk fluid temperature, T_b, i.e.

$$W_f(t) = hS[T_w(t) - T_b] \quad (7)$$

the heat balance equation (5) becomes

$$W(t) = hS[T_w(t) - T_b] + (\rho c_p V)_m \frac{dT_w}{dT}. \quad (8)$$

This equation may now be solved for the wall temperature distribution, T_w, using the stainless steel properties for the test section and equation (3), or equation (4), for the test section input power distribution. It was solved numerically by means of the ANATRA code [23], which will be briefly described afterwards. Parameters λ_1 and λ_2 in equation (4) (step power variations) have the physical meaning of the inverse of time constants of the electric feeding system which can be represented by two in-series delay blocks (each of them with a transfer function characterized by a pole of multiplicity two).

In the case of ramp power variations, equation (5), the electric feeding system can be represented by a single delay block of the same kind, characterized by λ.

The time-dependent expression of mass flux, $G(t)$, was derived by analogy from power time-dependent laws.

In this case parameters β_1 and β_2 in equation (2) and B in equation (3) have no direct physical meaning in the present analysis.

The numerical values of β_1, β_2, B, p_∞, λ_1, λ_2, and λ, were obtained first by equating equations (2)–(5) to the measured values of $G(t)$, $p(t)$ and $W(t)$, and then by applying a best-fit procedure.

Experimental uncertainty

An evaluation of the experimental uncertainty was achieved through carrying out 20 runs of the same test.

(a) Two parameter tests (flow rate/pressure): experimental result of time-to-crisis lie around the mean value (1.5 s) with a standard deviation of 0.05 s, and with a maximum deviation of ± 0.1 s.

(b) Three parameter tests: experimental results of time-to-crisis lie around the mean value (1.25 s) with a standard deviation of 0.035 s, and with a maximum deviation of ± 0.07 s.

Transient critical heat flux experiments results

The complete data set of experimental results is collected in ref. [22]. Some CHF parameters in the following figures, refer to 'steady-state conditions'. This is in the sense that they are computed, at inlet conditions, solving the equation systems given by the CISE-modified correlation—equation (1)—and time-dependent expressions of pressure, flow rate, and/or power variations (steady-state approach at inlet conditions).

(a) Transients caused by the simultaneous variation of flow rate and pressure

Experimental results are reported in Figs. 3 and 4, where the following are plotted:

- the ratio between the transient and the steady-state critical mass flux vs the depressurization rate (Fig. 3);

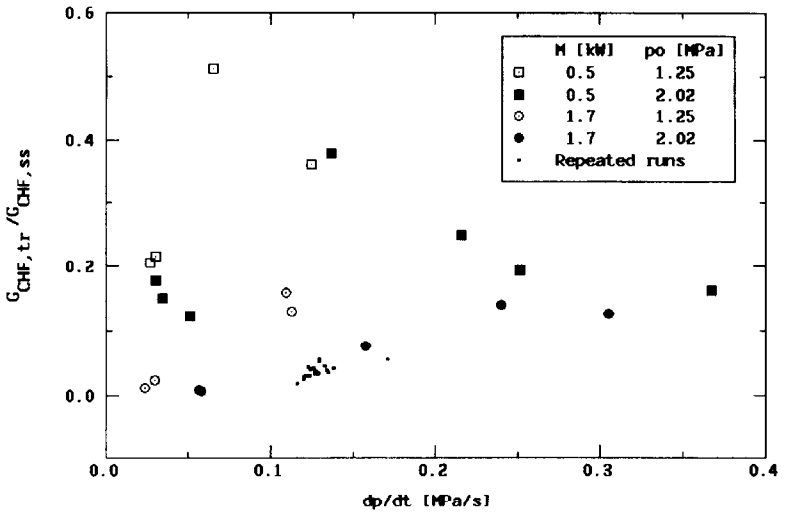

FIG. 3. Transient to steady-state critical mass flux vs the depressurization rate (pressure/flow rate transients).

● the ratio between the transient and the steady-state time-to-crisis vs the depressurization rate (Fig. 4).

From Fig. 3 it can be seen that the ratio $G_{CHF,tr}/G_{CHF,ss}$ shows a maximum, the value of which is a function of both M and p_o; for high values of the depressurization rate the ratio tends to a constant value. This trend is more pronounced with lower values of M and p_o, for which the maximum is obtained at lower values of dp/dt.

A similar behaviour, with the presence of a minimum, is shown by the ratio $t_{CHF,tr}/t_{CHF,ss}$ vs dp/dt.

As the ratio $G_{CHF,tr}/G_{CHF,ss}$ is always less than 1 (and the ratio $t_{CHF,tr}/t_{CHF,ss}$ is always greater than 1), this means that the CHF always occurs for values of time-to-crisis longer than those predicted with the steady-state approach at inlet conditions.

(b) Transients caused by the simultaneous variation of thermal power and pressure

Results regarding the step variation of the power are presented in Figs. 5 and 6, where the ratio between the transient and the steady-state critical thermal power and the ratio between the transient and the steady-state time-to-crisis are respectively plotted vs the depressurization rate, dp/dt.

The experimental time-to-crisis is greater than the steady-state value for very low dp/dt, then shows a minimum value and finally tends to increase again for high dp/dt.

In the region of the minimum value, the experimental time-to-crisis is less than the steady-state prediction. This behaviour may be qualitatively justified as follows.

For very small dp/dt, the CHF is delayed because of the energy storage in the wall thickness (then

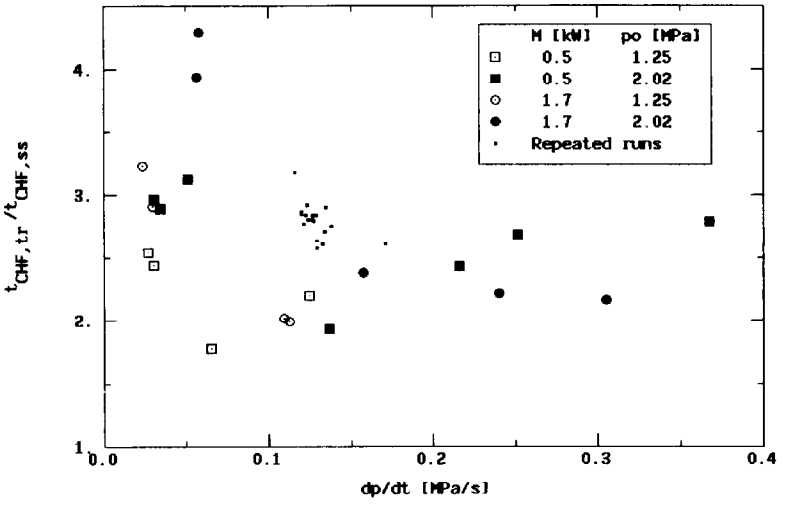

FIG. 4. Transient to steady-state time-to-crisis vs the depressurization rate (pressure/flow rate transients).

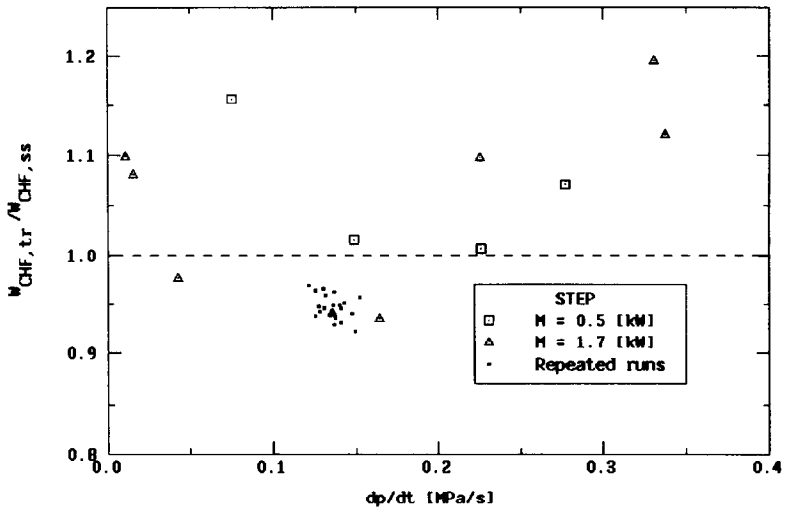

FIG. 5. Transient to steady-state critical thermal power vs the depressurization rate (pressure/step power transients).

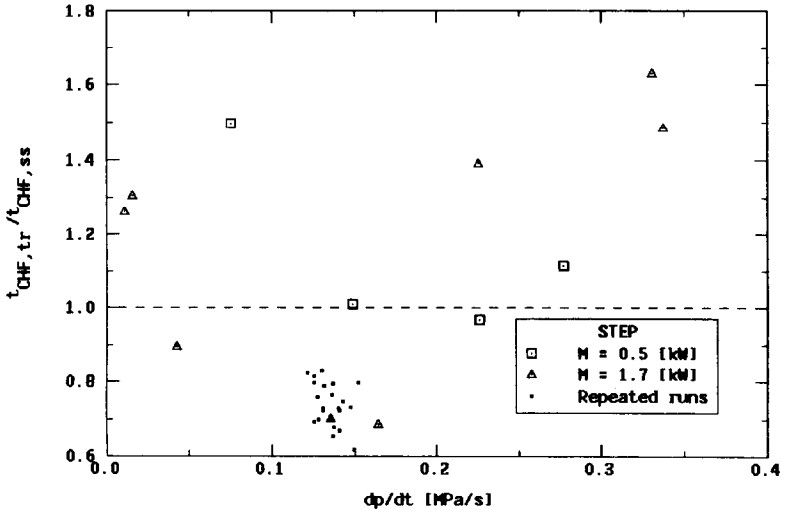

FIG. 6. Transient to steady-state time-to-crisis vs the depressurization rate (pressure/step power transients).

$t_{CHF,tr} > t_{CHF,ss}$). As dp/dt increases the actual thermal power delivered to the fluid increases because of the higher wall–fluid temperature difference due to the sudden depressurization [17]. Such a power increase tends to balance the delay of the CHF (sometimes it is predominant). Increasing the depressurization rate more and more we have an increase of outlet mass flow rate due to the sudden flow boiling. This aspect gives rise to a delay in the CHF because of the better cooling of the test section wall. For lower values of M, as the time-to-crisis is shorter, the influence of this latter phenomenon is less relevant.

Similar conclusions can be drawn from the tests carried out with ramp variations of the power, as shown in Figs. 7 and 8, where the ratio between the transient and the steady-state critical thermal power and the ratio between the transient and the steady-state time-to-crisis are respectively plotted vs the depressurization rate, dp/dt.

(c) Transients caused by the simultaneous variation of thermal power, flow rate and pressure

Experimental results are reported in Figs. 9(a)–(c) for step power variations and in Figs. 10(a)–(c) for ramp power variations. The following ratios are respectively plotted vs the depressurization rate, dp/dt:

- the ratio between the transient and the steady-state critical mass flux;
- the ratio between the transient and the steady-state critical thermal power;
- the ratio between the transient and the steady-state time-to-crisis.

From a macroscopic analysis of Figs. 9 and 10 it can be seen that the CHF occurs at longer values of the time-to-crisis than predicted by the steady-state approach at inlet conditions. That means lower values of the critical mass flux and higher values of the critical

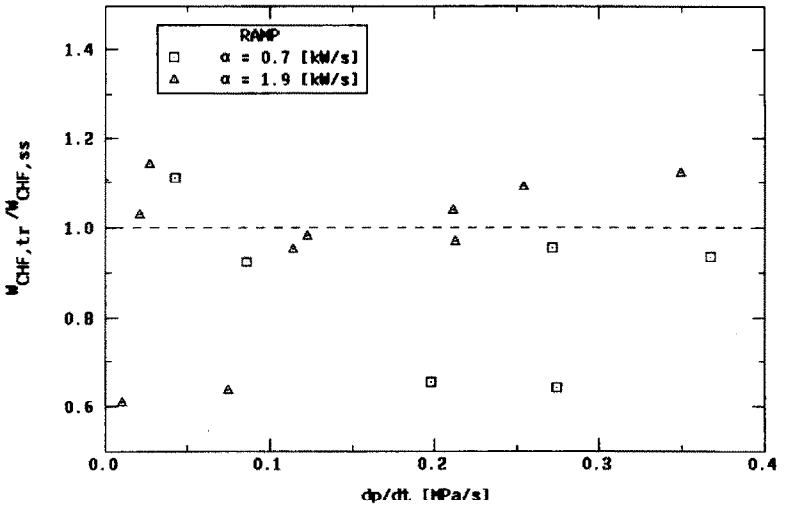

FIG. 7. Transient to steady-state critical thermal power vs the depressurization rate (pressure/ramp power transients).

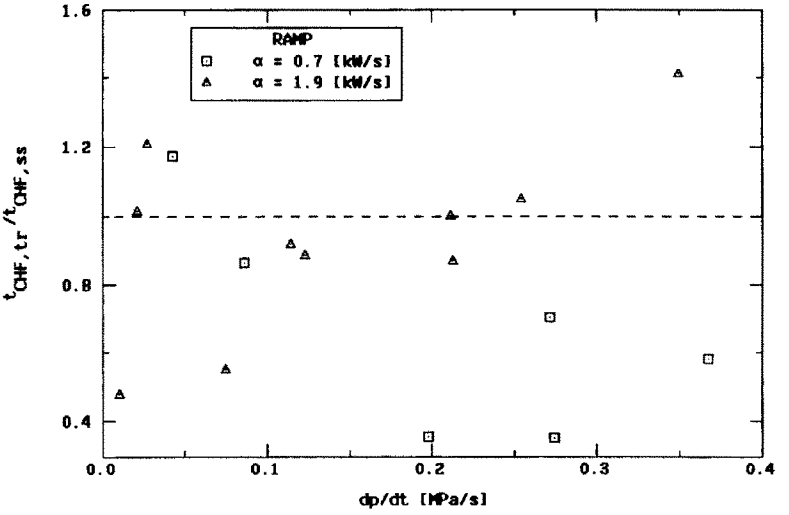

FIG. 8. Transient to steady-state time-to-crisis vs the depressurization rate (pressure/ramp power transients).

thermal power. The margin to the CHF, M, seems to affect the transient, whilst the influence of the system pressure can be neglected.

Also in this case there is a minimum in $t_{CHF,tr}/t_{CHF,ss}$ trend vs dp/dt as already observed in the previous subsection.

As a conclusion of this paragraph it is worth mentioning transients in which the power was varied alone or simultaneously with the flow rate but without pressure variations and transients caused by the simultaneous variation of power and pressure (independently from the variation of the flow rate).

In the first case [18, 19], there was a different behaviour depending on the kind of input power: step or ramp variation, the latter being a slower variation of the power and giving results intermediate between step variations and steady-state results.

In the case of simultaneous variation of power and pressure, ramp and step power variations can no longer be distinguished. This behaviour can be explained bearing in mind that, as shown in ref. [17], a pressure decrease gives rise to an increase of the local heat flux (thermal capacity of the wall) that must be summed up to the heat flux delivered to the fluid by the external heating. The local, transient heat flux, being sometimes very high, tends to minimize the difference between step and ramp variations making both very quick and very similar. In pressure transients [17], the local heat flux is responsible for the occurrence of the CHF only.

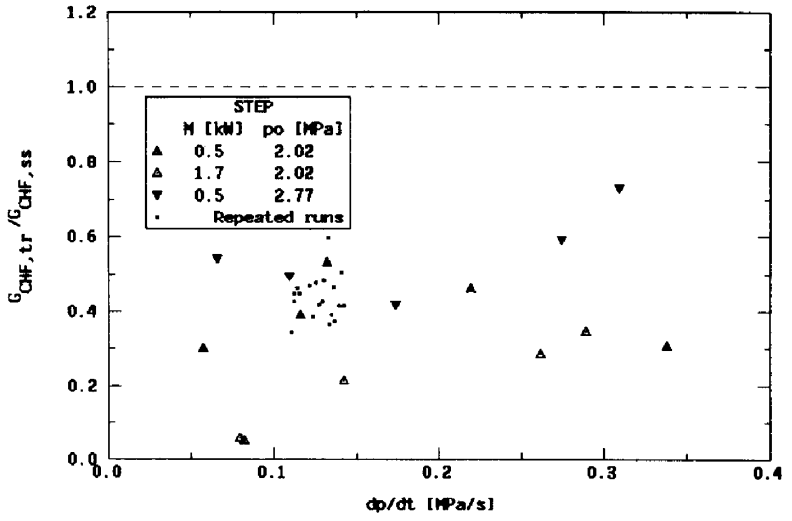

FIG. 9(a). Transient to steady-state critical mass flux vs the depressurization rate (pressure/flow rate/step power transients).

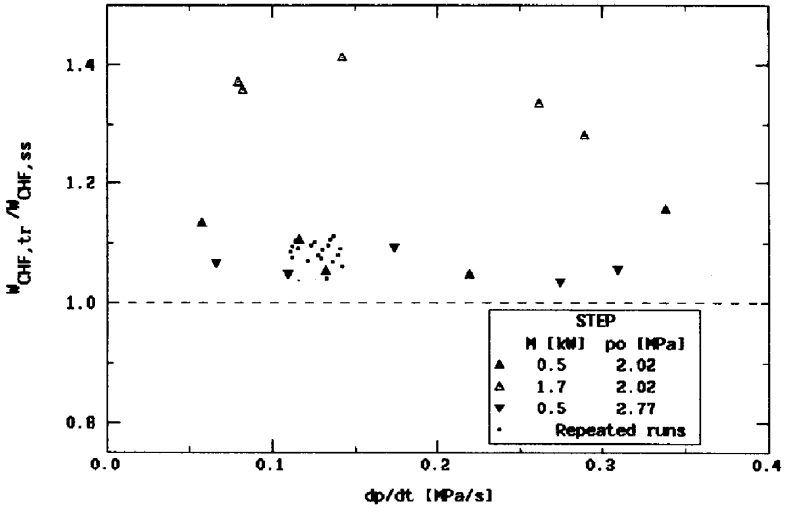

FIG. 9(b). Transient to steady-state critical thermal power vs the depressurization rate (pressure/flow rate/step power transients).

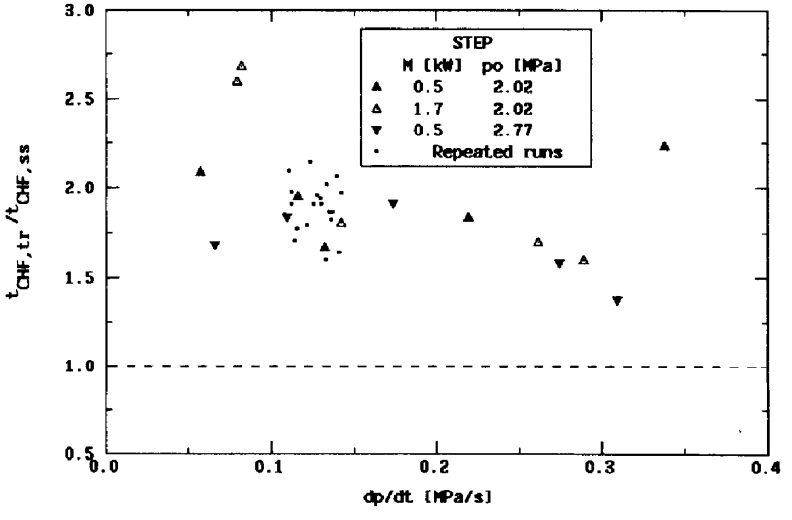

FIG. 9(c). Transient to steady-state time-to-crisis vs the depressurization rate (pressure/flow rate/step power transients).

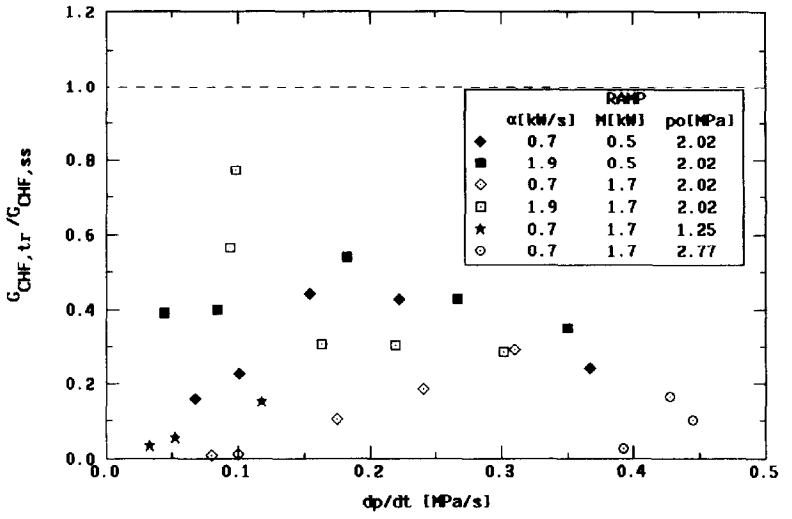

FIG. 10(a). Transient to steady-state critical mass flux vs the depressurization rate (pressure/flow rate/ramp power transients).

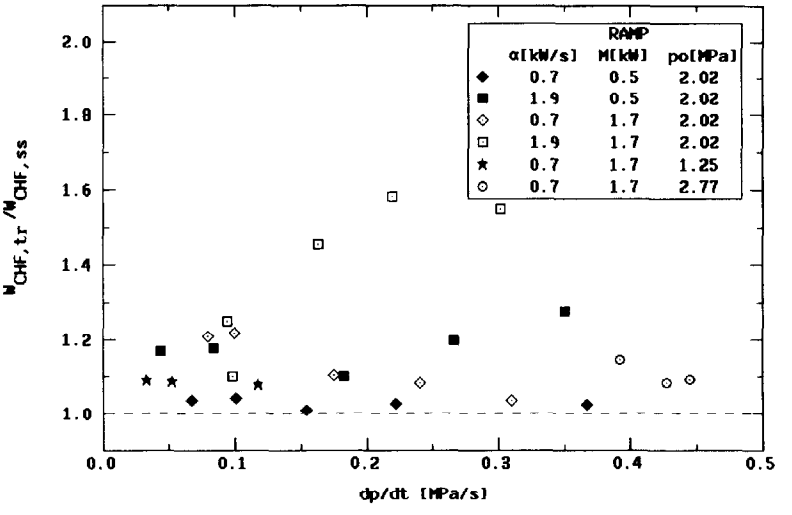

FIG. 10(b). Transient to steady-state critical thermal power vs the depressurization rate (pressure/flow rate/ramp power transients).

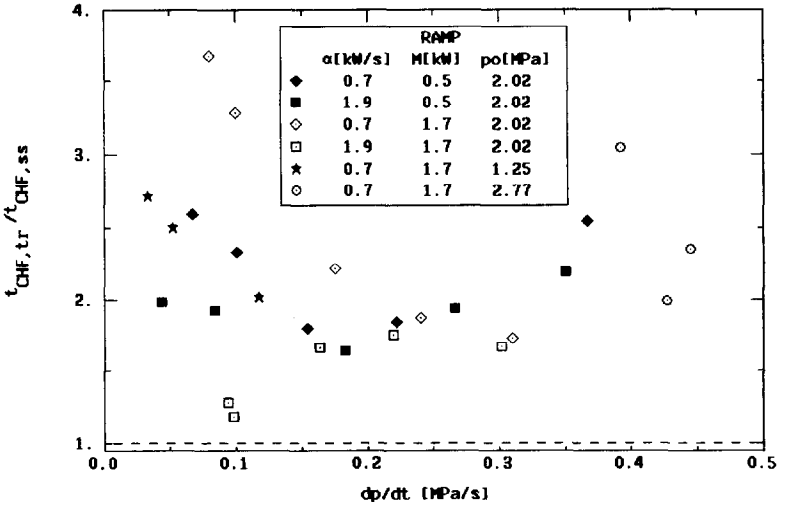

FIG. 10(c). Transient to steady-state time-to-crisis vs the depressurization rate (pressure/flow rate/ramp power transients).

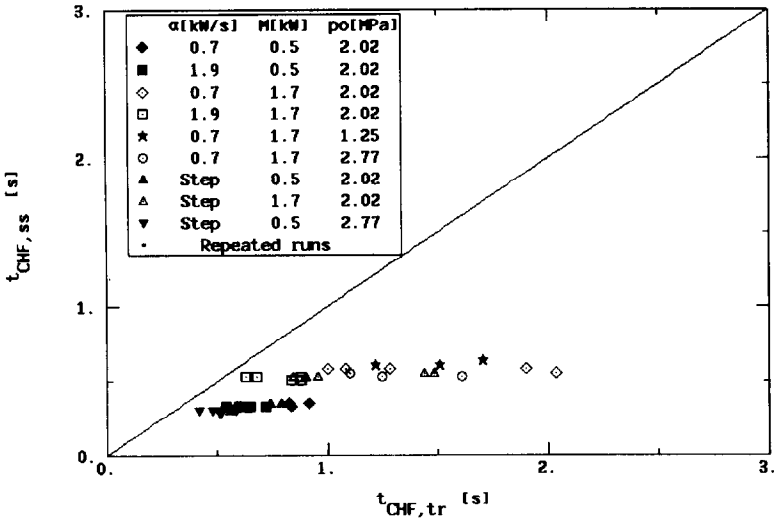

FIG. 11. Predictions of the time-to-crisis using the steady-state approach at inlet conditions (pressure/flow rate/power transients).

DATA ANALYSIS

In the previous paragraphs it has been shown how the steady-state approach at inlet conditions (i.e. the use of a steady-state correlation with the parameters calculated at the inlet section), is unable to predict transient CHF data. A summary of the results is presented in Fig. 11, where the steady-state time-to-crisis is plotted vs the transient time-to-crisis for flow rate/power/pressure transients.

It seems worth showing at this point a comparison between single (one-parameter) and multiple (two- or three-parameter) transients. In Fig. 12 this comparison is plotted for a typical flow variation. The superimposition of two or three variations gives rise to shorter actual time-to-crisis, whilst the steady-state value remains roughly constant. This was expected because the simultaneous occurrence of variations tending to induce boiling is obviously bound to give a synergic effect that brings forward the CHF condition.

As already stated in refs. [6, 19], in order to have a more realistic description of the phenomenon it is therefore necessary to examine the experimental data using the analysis of local conditions. A more suitable approach consists of using correlation (1) with the local instantaneous values of the parameters of interest. This method is sometimes called the 'quasi-steady-state' approach. To calculate the local conditions an original computer code was developed, ANATRA [23], based on heat transfer correlations reassessed by the authors [20]. ANATRA code is a HEM code one-dimensional in the fluid and two-dimensional in the wall thickness that solves the three balance equations applied for the test section with the finite differences method. The quasi-steady-state method for the prediction of CHF conditions consists of calculating the

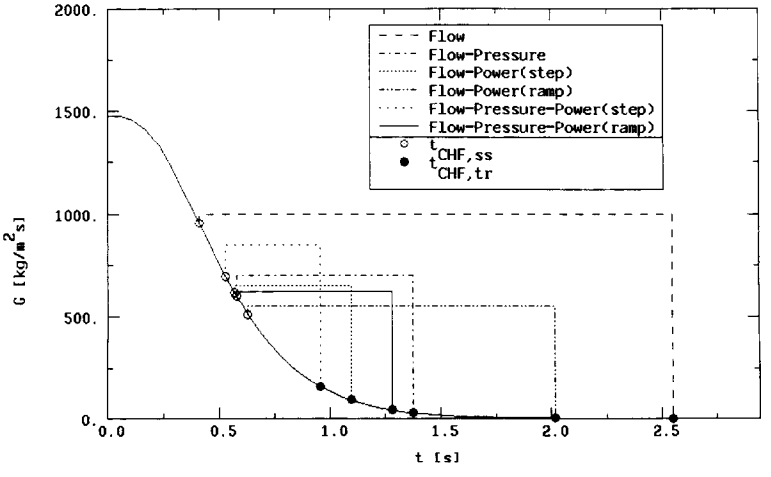

FIG. 12. Analysis of the effect on the CHF of the simultaneous occurrence of flow rate, pressure and power variations, with reference to single flow rate variations.

value of the local heat flux (or steam quality) every time-step and comparing the computed value with the prediction obtained using correlation (1) (or other equivalent reliable correlations). The CHF condition is indicated when the local value of the heat flux (or steam quality) is greater or equal to the value given by correlation (1).

A graphic representation of local condition analysis is reported in Figs. 13–15, respectively, for pressure/flow rate, pressure/power and pressure/power flow rate transients. In each figure the following are plotted:

(a) the calculated vs the experimental time-to-crisis;

(b) the ratio between the calculated and the experimental time-to-crisis vs the depressurization rate, dp/dt.

Most data lie within a $\pm 25\%$ band without any significant systematic deviation, and that must be considered a positive result. Larger deviations are observed for data characterized by fast variations of the pressure, coupled with low margin to crisis, M. It is possible to fix a threshold of the depressurization rate beyond which the quasi-steady-state approach is no longer adequate for prediction of the transient CHF: 0.2 MPa s^{-1}.

In ref. [17] it was clearly shown how, because of the wall thickness thermal capacity, a pressure transient in a two-phase mixture under saturated conditions produces a very steep power transient, much faster than the step power variation carried out in the experiments.

Under very fast transient conditions several

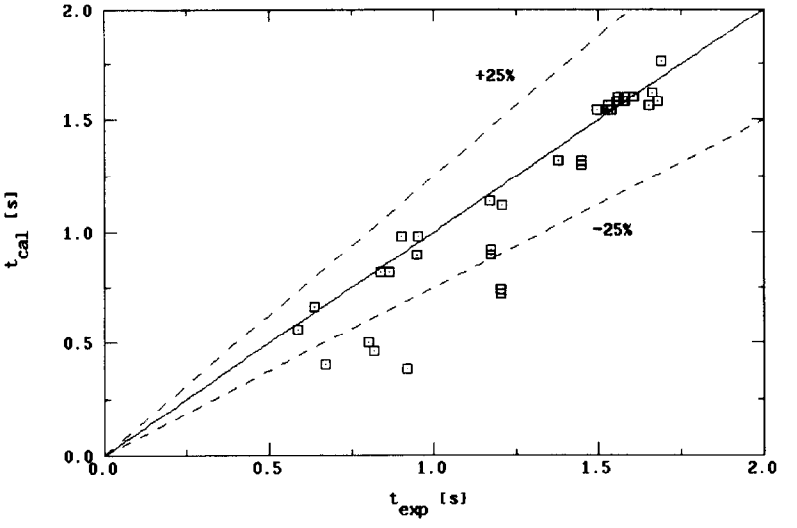

FIG. 13(a). Predictions of the time-to-crisis using the ANATRA code (pressure/flow rate transients).

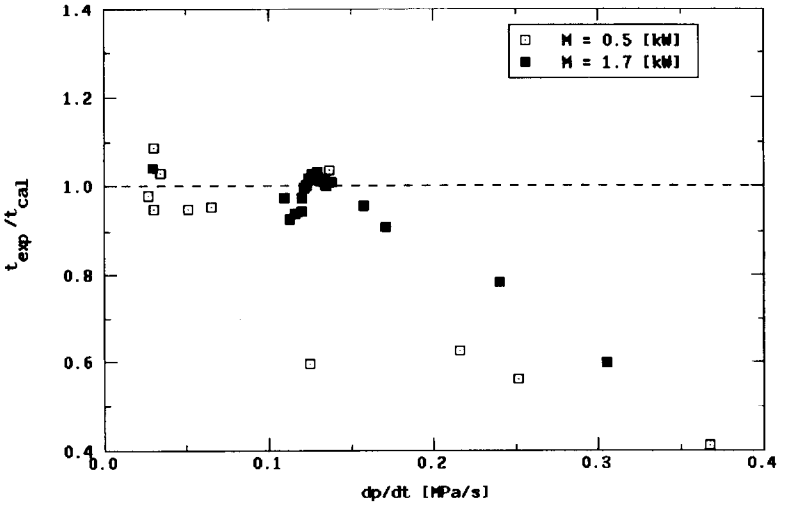

FIG. 13(b). Influence of the depressurization rate on ANATRA predictions (pressure/flow rate transients).

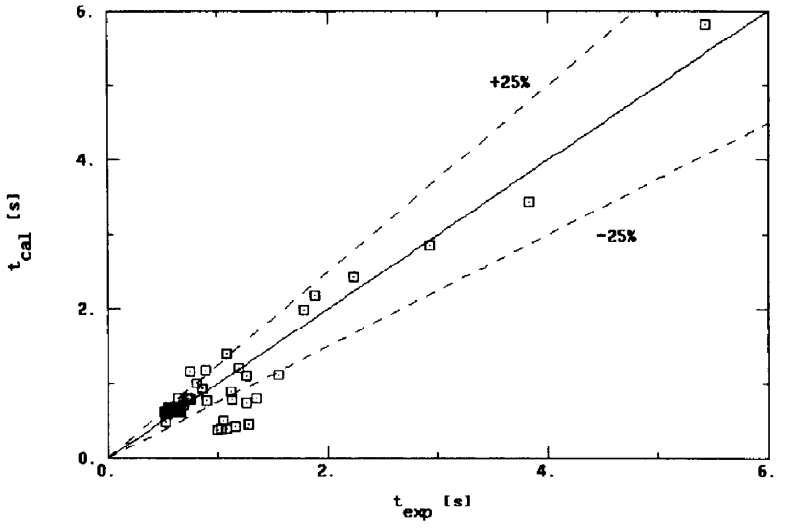

FIG. 14(a). Predictions of the time-to-crisis using the ANATRA code (pressure/power transients).

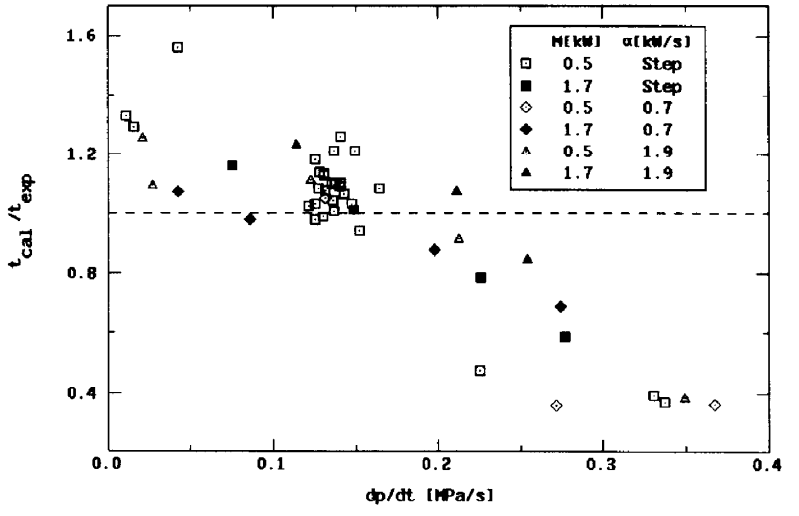

FIG. 14(b). Influence of the depressurization rate on ANATRA predictions (pressure/power transients).

hypotheses are no longer adequate:

- the homogeneous equilibrium model (slip and thermal disequilibrium during vaporization);
- the assumptions made in the numerical solution.

In addition the quasi-steady-state approach may be valid only if the heat capacity of the solid is much greater than the heat capacity of the fluid; this means that the response time of the fluid (convective time constant) is much smaller than the response time of the wall [24, 25].

On the other hand, taking into account such aspects would make the ANATRA code similar to existing and more sophisticated system codes (e.g. TRAC).

The biggest advantage in making use of the ANATRA code is its simplicity (in comparison with TRAC or RELAP codes) and capability of predicting with a good accuracy almost the whole range of variations investigated. It is worthwhile stressing here that very fast pressure transients are of little practical significance. However, they allowed us to establish the limits of the quasi-steady-state approach and homogeneous equilibrium model.

SUMMARY AND CONCLUSIONS

An experimental investigation of CHF behaviour during transients caused by the simultaneous occurrence of pressure, flow rate and/or power variations using R-12 in a vertical heated channel was performed.

The experimental data revealed the general inadequacy of using the steady-state CHF correlations at inlet conditions in predicting transient situations.

An analysis of the local conditions together with

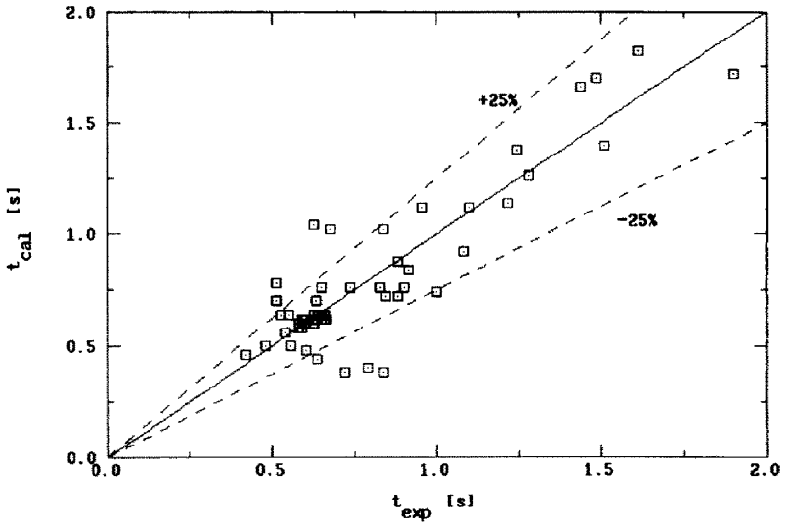

FIG. 15(a). Predictions of the time-to-crisis using the ANATRA code (pressure/power/flow rate transients).

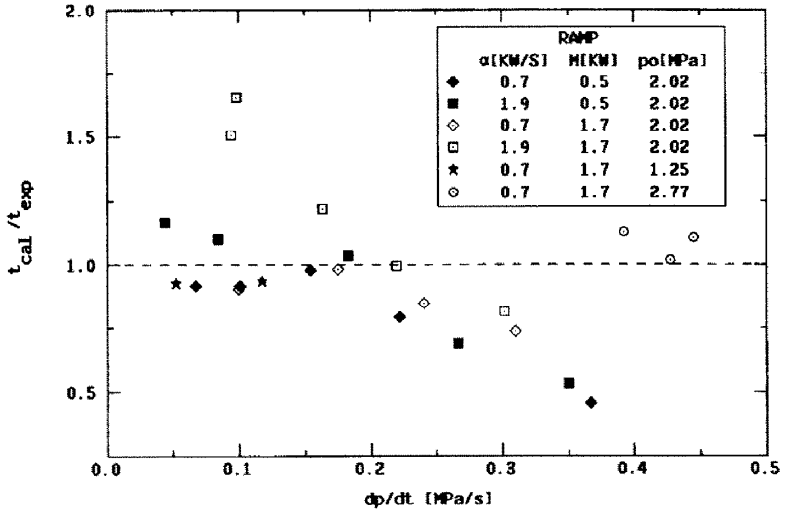

FIG. 15(b). Influence of the depressurization rate on ANATRA predictions (pressure/power flow rate transients).

the adoption of the quasi-steady-state approach is shown to estimate the experimental data reasonably well, with an uncertainty of $\pm 20\%$ for most tests. The verdict on the method must be favourable. The disagreement with very fast pressure variations experimental data is of little practical significance. Nevertheless it is useful to establish the limits of the HEM and the quasi-steady-state method in the prediction of the CHF under transient conditions.

Acknowledgements—The authors are deeply grateful to G. Farina, M. Morlacca and A. Lattanzi who performed the experimental runs.

REFERENCES

1. J. C. Collier, *Convective Boiling and Condensation*, 2nd Edn, pp. 248–313. McGraw-Hill, New York (1972).
2. A. E. Bergles, J. G. Collier, J. M. Delhaye, G. F. Hewitt and F. Mayinger, *Two-phase Flow and Heat Transfer in the Power and Process Industries*, pp. 256–280. Hemisphere, Washington, DC (1981).
3. G. F. Hewitt, Burnout. In *Handbook of Multiphase Systems* (Edited by G. Hetsroni). Hemisphere, Washington, DC (1982).
4. Y. Katto, Forced-convection boiling in uniformly heated channels. In *Handbook of Heat and Mass Transfer* (Edited by N. P. Cheremisinoff), pp. 303–325. Gulf, Houston (1986).

5. Y. Katto, Critical heat flux in boiling, *Proc. 8th Int. Heat Transfer Conf.*, Vol. 1, pp. 171–180. Hemisphere, Washington, DC (1986).
6. I. Kataoka and A. Serizawa, Transient boiling heat transfer under forced convection. In *Handbook of Heat and Mass Transfer* (Edited by N. P. Cheremisinoff), pp. 327–383. Gulf, Houston (1986).
7. D. Moxon and P. A. Edwards, Dryout during flow and power transient, *Proc. European Two-phase Flow Group Meeting*. Winfrith, U.K. (June 1967).
8. G. P. Gaspari, R. Granzini and A. Hassid, Dryout onset in flow stoppage, depressurization and power surge transients, *Energia Nucleare* **20,** 554 (1973).
9. B. S. Shiralkar, E. E. Polomik, R. T. Lahey, J. M. Gonzales, D. W. Radcliffe and L. E. Schnebly, Transient critical heat flux—experimental results, General Electric Report, GEAP 13295 (1972).
10. O. K. Smirnov, L. T. Pashkov and V. N. Zaitsev, Investigation of critical heat flux with decrease in flow through a heated tube, *Teploenergetika* **19,** 83 (1972).
11. O. K. Smirnov, V. N. Zaitsev and E. E. Serov, Investigation of burnout under transient hydrodynamic conditions, *Teploenergetika* **24,** 81 (1977).
12. T. Iwamura and T. Kuroyanagi, Burnout characteristics under flow reduction condition, *J. Nucl. Sci. Technol.* **19,** 438 (1982).
13. M. Cumo, F. Fabrizi and G. Palazzi, Transient critical heat flux in loss of flow transients, *Int. J. Multiphase Flow* **4,** 497–509 (1978).
14. J. C. M. Leung, Transient critical heat flux and blowdown heat transfer studies, ANL Report, ANL-80-53, NUREG/CR, 1559 (1980).
15. J. C. M. Leung, Occurrence of critical heat flux during blowdown with flow reversal, ANL Report, ANL-77-4 (1977).
16. G. P. Celata, M. Cumo, F. D'Annibale, G. E. Farello and T. Setaro, Flow transients experiments with refrigerant-12, *Revue Gen. Thermique* **XXV**(299), 513–519 (1986) (also as Report RT/TERM 86/2).
17. G. P. Celata, M. Cumo, F. D'Annibale and G. E. Farello, CHF in flow boiling during pressure transients. In *Particulate Phenomena and Multi-phase Transport* (Edited by T. N. Veziroglu), Vol. 2, pp. 207–223. Hemisphere, Washington, DC (1988).
18. G. P. Celata, M. Cumo, F. D'Annibale, G. E. Farello and S. A. Said, Critical heat flux phenomena in flow boiling during step-wise and ramp-wise power transients, *Revue Gen. Thermique* No. 317, 296–303 (June 1988) (also as ENEA Report RT/TERM 87/3).
19. G. P. Celata, M. Cumo, F. D'Annibale and G. E. Farello, Transient CHF in flow boiling during flow rate and thermal power simultaneous variations, *Exp. Thermal Fluid Sci.* **2**(2), 134–145 (1989) (also as ENEA Report RT/TERM 88/5).
20. G. P. Celata, M. Cumo, F. D'Annibale, G. E. Farello and T. Setaro, Reassessment of forced convection heat transfer correlations for refrigerant-12, *Energia Nucleare* **3**(4), 19–32 (April 1986).
21. S. Bertoletti, G. P. Gaspari, C. Lombardi, G. Peterlongo and M. Sivestri, Heat transfer crisis with steam–water mixtures, *Energia Nucleare* **12**(13), 121–172 (1965).
22. G. P. Celata, M. Cumo, F. D'Annibale and G. E. Farello, A data set of critical heat flux of boiling R-12 in uniformly heated vertical tubes under transient conditions, ENEA Report RT/TERM 89/2 (1989).
23. G. P. Celata, M. Cumo, F. D'Annibale, G. E. Farello and S. A. Said, ANATRA—a computer code for transient critical heat flux analysis with refrigerant-12, ENEA Report NQDU 1TS4B89048 (1989).
24. H. Kawamura, Experimental and analytical study of transient heat transfer for turbulent flow in a circular tube, *Int. J. Heat Mass Transfer* **20,** 443–449 (1977).
25. J. Sucec, An improved quasi-steady approach for transient conjugated forced convection problems, *Int. J. Heat Mass Transfer* **24,** 1711–1722 (1981).

COMPORTEMENT CHF PENDANT DES VARIATIONS SIMULTANEES DE PRESSION, PUISSANCE ET/OU DEBIT-MASSE

Résumé—On rapporte les résultats d'une étude expérimentale sur le flux thermique critique dans l'ébullition en convection forcée pendant des régimes transitoires causés par des variations simultanées de soit deux, soit trois paramètres parmi pression, débit-masse et puissance thermique. Les trois paramètres varient suivant une loi exponentielle pour le débit et la dépressurisation et suivant une rampe ou un échelon pour l'accroissement de puissance. Les expériences concernent une section tubulaire d'essai qui est électriquement et uniformément chauffée. Les paramètres incluent le débit à mi-variation de débit dans le temps, plusieurs valeurs de la puissance initiale (avant la variation) et la puissance finale (après la variation) dans le cas de l'échelon, et la pente de la rampe dans le cas correspondant, et le taux de dépressurisation. Une analyse des données expérimentales est conduite par une approche des conditions locales et en appliquant la méthode de l'état quasi-statique. L'effet de la variation simultanée de deux ou trois paramètres principaux sur le temps d'apparition de la crise est analysé pou des transitoires dans lesquels un seul paramètre varie.

DAS VERHALTEN DER KRITISCHEN WÄRMESTROMDICHTE (CHF) BEI GLEICHZEITIGEN VERÄNDERUNGEN VON DRUCK, WÄRMESTROMDICHTE UND/ODER MASSENSTROMDICHTE

Zusammenfassung—In der vorliegenden Arbeit werden die Ergebnisse einer experimentellen Untersuchung der kritischen Wärmestromdichte beim Strömungssieden unter instationären Bedingungen vorgestellt. Hierbei werden zwei der folgenden Parameter gleichzeitig variiert: Druck, Massenstromdichte und Wärmestromdichte. Die Veränderungen der Massenstromdichte und des Drucks erfolgen exponentiell, diejenigen der Wärmestromdichte rampenförmig oder sprungförmig. Die Experimente werden in einer gleichmäßig elektrisch beheizten, rohrförmigen Meßstrecke ausgeführt. Die Versuchsparameter umfassen folgende Werte: die Halbwertszeit der Massenstromdichte, einige Werte der Wärmestromdichte (vor Einsetzen der transienten Änderungen) sowie die Wärmestromdichte am Ende der Transienten für den Fall von stufenweisen Veränderungen, die Form der Rampe im Fall rampenförmiger Veränderungen, die Geschwindigkeit der Druckabsenkung. Das experimentelle Datenmaterial wird analysiert, wobei eine Näherung für die örtlichen Bedingungen und ein quasi-stationäres Verfahren angewandt wird. Der Einfluß der gleichzeitigen Variation von zwei oder drei Hauptparametern auf die Zeit bis zum Einsetzen der Siedekrise wird auch für solche Transienten untersucht, bei denen nur ein Parameter verändert wird.

ПОВЕДЕНИЕ КРИТИЧЕСКОГО ТЕПЛОВОГО ПОТОКА ПРИ ОДНОВРЕМЕННЫХ ИЗМЕНЕНИЯХ ДАВЛЕНИЯ, МОЩНОСТИ И/ИЛИ СКОРОСТИ ТЕЧЕНИЯ

Аннотация—Приводятся результаты экспериментального исследования критического теплового потока в переходном режиме кипения при вынужденной конвекции, которые вызваны одновременными изменениями двух или трех параметров, включающих давление, скорость течения и тепловую мощность. Три указанных параметра варьируются в соответствии с экспоненциальным законом при уменьшении скорости течения и давления, а также в соответствии с законом скачкообразного или плавного перехода при увеличении подводимой мощности. Эксперименты проводились на цилиндрическом опытном участке, однородно нагреваемом электрическим током. Экспериментальные параметры включали время затухания скорости течения на половине его пути, несколько значений начальной (перед переходом) и конечной (в конце перехода) мощности в случае скачкообразных переходов, угол наклона в случае плавных переходов, а также интенсивность сброса давления. Экспериментальные данные анализируются с использованием методов локальных условий и квазистационарного. Влияние одновременных изменений двух или трех основных параметров на время до наступления кризиса анализируется также для переходов, при которых варьируется лишь один параметр.